IEEE Photonics Journal
An IEEE Photonics Society Publication

Open Access

Employing Hybrid sub-Nyquist Sampling Rates to Support Heterogeneous Services of Varying Capacity in 25-Gbps DDM-OFDM-PON

Volume 10, Number 2, April 2018

Jhih-Hao Hsu
Min Yu
Chia-Chien Wei
Chi-Hsiang Lin
Chun-Ting Lin
Fumin Liu
Lei Zhou
LiMing Fang

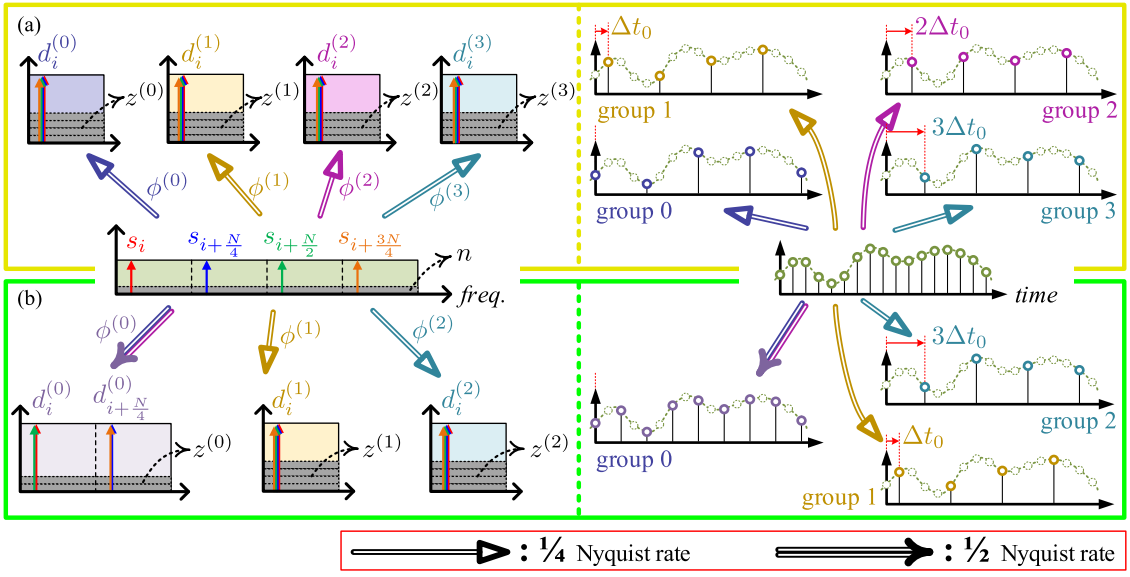

DOI: 10.1109/JPHOT.2018.2815619
1943-0655

Employing Hybrid sub-Nyquist Sampling Rates to Support Heterogeneous Services of Varying Capacity in 25-Gbps DDM-OFDM-PON

Jhih-Hao Hsu,[1] Min Yu,[1] Chia-Chien Wei,[1] Chi-Hsiang Lin,[2] Chun-Ting Lin,[2] Fumin Liu,[3] Lei Zhou,[3] and LiMing Fang[3]

[1]Department of Photonics, National Sun Yat-sen University, Kaohsiung 804, Taiwan
[2]Institute of Photonic System, National Chiao Tung University, Tainan 711, Taiwan
[3]Advanced Optical Access Network Research Center, Huawei Technologies, Shenzhen 518000, China

DOI:10.1109/JPHOT.2018.2815619

Manuscript received January 9, 2018; revised March 7, 2018; accepted March 8, 2018. Date of publication March 13, 2018; date of current version April 2, 2018. Corresponding author: Chia-Chien Wei (e-mail: ccwei@mail.nsysu.edu.tw).

Abstract: Delay-division-multiplexing (DDM) involves the use of signal preprocessing for the detection of data via sub-Nyquist analog-to-digital sampling, based on preallocated relative sampling delays among optical network users (ONUs) in an orthogonal frequency-division multiplexing (OFDM) passive optical network (PON). If a DDM-PON consists of M virtual groups, the sampling rate at the receivers is only $1/M$ of the Nyquist rate, but the maximum capacity of each ONU is fixed at $1/M$ of the total capacity. In this study, we developed a novel DDM scheme that uses hybrid sub-Nyquist sampling rates to accommodate heterogeneous services of different capacities in an OFDM-PON. To equalize the transmission performances using hybrid sub-Nyquist sampling rates, the modification of preprocessing was proposed, and its necessity was demonstrated. Without loss of generality, we experimentally demonstrated a 25-Gbps DDM-OFDM-PON using hybrid sampling at 1/2, 1/8, and 1/32 (or 1/8, 1/16, and 1/32) of the Nyquist rate. Compared to a DDM-PON with a fixed sub-Nyquist rate, the received signals based on hybrid sub-Nyquist sampling rates show similar sensitivities. A loss budget of 26 dB was experimentally achieved using all sub-Nyquist sampling rates after employing the modified preprocessing.

Index Terms: Delay-division multiplexing, sub-Nyquist sampling, orthogonal frequency-division multiplexing.

1. Introduction

Rapid growth in bandwidth-hungry applications has shifted the bandwidth bottleneck to metro and access networks. Passive optical network (PON) technology is regarded as a promising candidate for internet access, thanks to its high capacity and low cost. Advancements in digital signal processing (DSP) have brought orthogonal frequency-division multiplexing (OFDM) to the forefront of high-speed networks. Time-division multiple access (TDMA) and orthogonal frequency-division multiple access (OFDMA) both require high aggregated downstream data rates for OFDM-PON, due to the fact that it is shared by multiple optical network users (ONUs) [1]–[3]. As a result, ONUs in an OFDM-PON require an analog-to-digital converter (ADC) with a high sampling rate (i.e., $\geq$

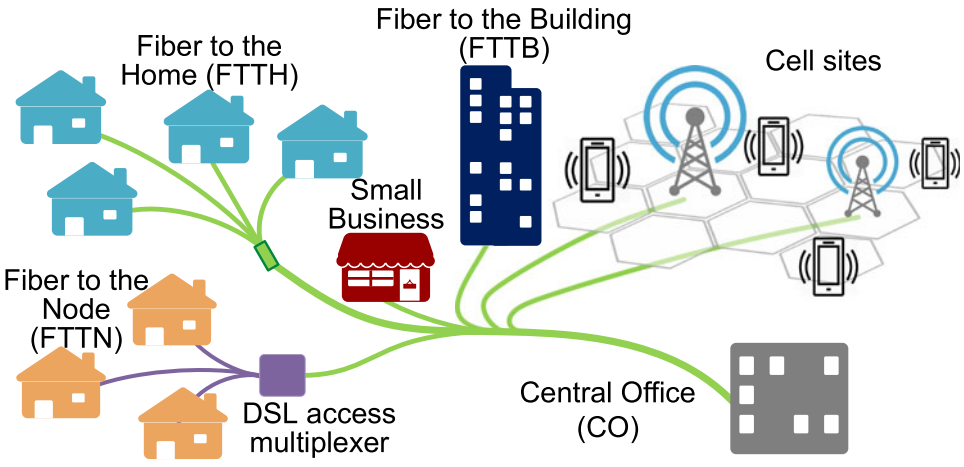

Fig. 1. Architecture of heterogeneous PON.

Nyquist rate), even though they use only a small portion of the data. Delay-division multiplexing (DDM) based on sub-Nyquist sampling was developed to allow the use of ADCs with lower sampling rates [4], [5]. The necessary sampling rate can be reduced to only $1/M$ of the Nyquist rate when the ONUs are classified into M virtual groups.

Numerous methods have been developed for last-mile access, including wireless technologies, fiber-to-the-home (FTTH), and copper-based digital subscriber lines (DSL), and PONs must be able to accommodate all of these heterogeneous access techniques [6], [7]. In this scenario, the central office (CO) sends data to heterogeneous ONUs for internet connections and mobile backhauling [8], [9], as shown in Fig. 1. In contrast, a DDM-OFDM-PON based on ADCs operating at $1/M$ of the Nyquist rate limits the maximum received capacity values of all ONUs to the same level (i.e., $1/M$ of the downstream capacity) [4], [5]. Such limitations are ill-suited to ONUs with heterogeneous characteristics, such as enterprise users requiring higher capacities.

In this paper, we propose a novel DDM-OFDM-PON in which different ONUs can use ADCs with different sub-Nyquist sampling rates in order to enhance the flexibility of bandwidth sharing. For example, ADCs can be assigned higher sub-Nyquist rates for ONUs requiring higher capacities. We also propose modification of the pre-processing of downstream data at the CO in order to equalize the received signal performance for all ONUs. Thus, it is possible to receive data of various bandwidths at similar sensitivities in the proposed system, without the need for an additional DSP at receivers. In experiments, we demonstrated 25-Gbps downstream transmission using a modulation format of 16 quadrature amplitude modulation (QAM) in a DDM-OFDM-PON, where the Nyquist rate was 14 GSa/s and the total bandwidth was 7 GHz. Unlike the p-i-n photodiode employed in [4], [5], we adopted an avalanche photodiode (APD) to enhance the power budget [10]. Based on hybrid sampling at 1/2, 1/8 and 1/32 (or 1/8, 1/16 and 1/32) of the Nyquist rate, the modified pre-processing scheme allowed for a loss budget of 26 dB for all of the sampling rates in a 25-km APD-based DDM transmission system.

2. Concept of Hybrid Sub-Nyquist Sampling

In the existing DDM scheme [5], spectral aliasing based on $1/M$ of the Nyquist rate makes each received subcarrier the superposition of M sent subcarriers. A suitable degree of variation in the sampling delays among M virtual groups makes it possible to obtain M independent aliasing results [5]. Thus, the received ith subcarrier of the mth group can be derived as follows:

$$r_i^{(m)} = \sum_{l=0}^{M-1} \exp\left(j\phi_{k[l]}^{(m)}\right) \times \left(h_{k[l]}^{(m)} \cdot s_{k[l]} + n_{k[l]}\right), \tag{1}$$

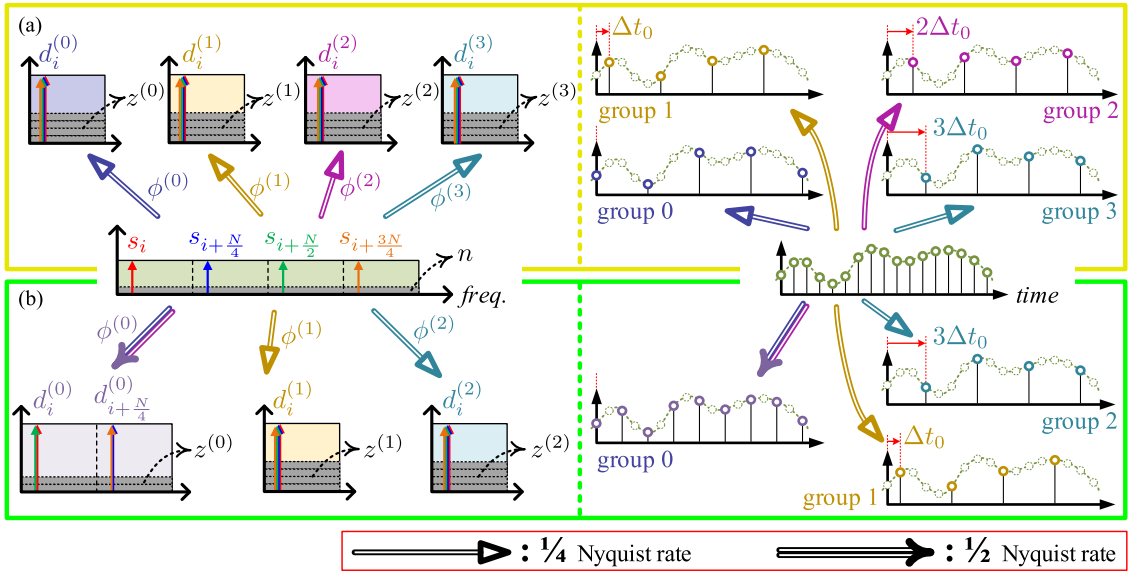

Fig. 2. Concept of DDM with (a) fixed sub-Nyquist sampling rates and (b) hybrid sub-Nyquist sampling rates (left column: the frequency domain; right column: the time domain).

where s, n, h and ϕ respectively denote the sent subcarrier, additive noise, channel response and the phase induced by sampling delay. Note that the channel response h excludes the phase shift caused by sampling delay. Subscript $k[l]$ as a function of l indicates that the parameters in (1) are associated with the $(i + l \times N/M)$th sent subcarrier, where N is the number of total subcarriers. In accordance with (1), it is the difference in the sampling delay that enables different subcarriers to be received by different groups. For the sake of simplicity, the channel responses to each group are similar; i.e., $h^{(m)}_{k[l]} \approx h_{k[l]}$. Dividing transmitted information into M parts without data loss involves the selection of sampling delays such that all sub-Nyquist samples form Nyquist samples via time-interleaving [5], as shown in Fig. 2(a) where M is set at 4. In other words, if Δt_0 denotes the reciprocal of the Nyquist rate (i.e., $1/\Delta t_0 = 2\pi/N$), then the sampling delay associated with the mth group would be set at $m\Delta t_0$, which would result in [5],

$$\phi^{(m)}_{k[l]} = k[l] \times m\Delta t_0 = \frac{2m\pi k[l]}{N} = \frac{2m\pi i}{N} + \frac{2m\pi l}{M} = \phi^{(m)}_i + l \times \frac{2m\pi}{M}. \tag{2}$$

Thus, with the ideal sampling delays in Fig. 2(a), $r^{(m)}_i$ can be summarized in matrix form as follows:

$$\begin{bmatrix} r^{(0)}_i \\ r^{(1)}_i \\ r^{(2)}_i \\ r^{(3)}_i \end{bmatrix} = \underbrace{\begin{bmatrix} e^{j\phi^{(0)}_i} & 0 & 0 & 0 \\ 0 & e^{j\phi^{(1)}_i} & 0 & 0 \\ 0 & 0 & e^{j\phi^{(2)}_i} & 0 \\ 0 & 0 & 0 & e^{j\phi^{(3)}_i} \end{bmatrix} \begin{bmatrix} 1 & 1 & 1 & 1 \\ 1 & j & -1 & -j \\ 1 & -1 & 1 & -1 \\ 1 & -j & -1 & j \end{bmatrix}}_{\Phi} \tag{3}$$

$$\times \left(\begin{bmatrix} h_i & 0 & 0 & 0 \\ 0 & h_{i+\frac{N}{4}} & 0 & 0 \\ 0 & 0 & h_{i+\frac{N}{2}} & 0 \\ 0 & 0 & 0 & h_{i+\frac{3N}{4}} \end{bmatrix} \begin{bmatrix} s_i \\ s_{i+\frac{N}{4}} \\ s_{i+\frac{N}{2}} \\ s_{i+\frac{3N}{4}} \end{bmatrix} + \begin{bmatrix} n_i \\ n_{i+\frac{N}{4}} \\ n_{i+\frac{N}{2}} \\ n_{i+\frac{3N}{4}} \end{bmatrix} \right) = \begin{bmatrix} d^{(0)}_i \\ d^{(1)}_i \\ d^{(2)}_i \\ d^{(3)}_i \end{bmatrix} + \begin{bmatrix} z^{(0)}_i \\ z^{(1)}_i \\ z^{(2)}_i \\ z^{(3)}_i \end{bmatrix},$$

(i.e., $\mathbf{r} = \Phi(\mathbf{Hs} + \mathbf{n}) = \mathbf{d} + \mathbf{z}$), where $\Phi = \left[\exp\left(j\phi_{k[l]}^{(m)}\right)\right]$ is an $M \times M$ matrix, and z denotes the received noise. If $d_i^{(m)}$ in (3) equals the data demanded by ONUs, the pre-processing of $\mathbf{s} = \mathbf{H}^{-1}\Phi^{-1}\mathbf{d}$ is required at CO. As in [5], sub-Nyquist sampling with appropriate pre-processing and sampling delays would lead to insignificant penalty in a DDM-PON, compared to the Nyquist sampling in a traditional OFDM-PON. In the proposed DDM-PON with hybrid sub-Nyquist sampling rates, the number of groups with $1/M_p$ of the Nyquist rate is L_p, thereby requiring that

$$\sum_{p=0}^{P-1} \frac{L_p}{M_p} = 1, \tag{4}$$

where P is the number of different sub-Nyquist rates in a DDM-PON. Fig. 2(b) extends the example in Fig. 2(a) to our proposed scheme where $P = 2$, $(1/M_0, 1/M_1) = (1/2, 1/4)$, and $(L_0, L_1) = (1, 2)$. Obviously, a higher sampling rate (e.g., the 0th group in Fig. 2(b)) would result in less aliasing and a greater number of received subcarriers. To make full use of the sent information without data loss requires that the sub-Nyquist samples received by the 0th group in Fig. 2(b) comprise the sub-Nyquist samples received by the 0th and 2nd groups in Fig. 2(a). Thus, if the sampling delay for the 0th group in Fig. 2(b) is 0, then the delays for the 1st and 2nd groups in Fig. 2(b) should be Δt_0 and $3\Delta t_0$, respectively. In this case when using hybrid sampling rates, (3) could be rewritten as follows:

$$\begin{bmatrix} r_i^{(0)} \\ r_{i+\frac{N}{4}}^{(0)} \\ r_i^{(1)} \\ r_i^{(2)} \end{bmatrix} = \underbrace{\begin{bmatrix} e^{j\phi_i^{(0)}} & 0 & 0 & 0 \\ 0 & e^{j\phi_i^{(0)}} & 0 & 0 \\ 0 & 0 & e^{j\phi_i^{(1)}} & 0 \\ 0 & 0 & 0 & e^{j\phi_i^{(2)}} \end{bmatrix} \begin{bmatrix} 1 & 0 & 1 & 0 \\ 0 & 1 & 0 & 1 \\ 1 & j & -1 & -j \\ 1 & -j & -1 & j \end{bmatrix}}_{\Phi} \tag{5}$$

$$\times \left(\begin{bmatrix} h_i & 0 & 0 & 0 \\ 0 & h_{i+\frac{N}{4}} & 0 & 0 \\ 0 & 0 & h_{i+\frac{N}{2}} & 0 \\ 0 & 0 & 0 & h_{i+\frac{3N}{4}} \end{bmatrix} \begin{bmatrix} s_i \\ s_{i+\frac{N}{4}} \\ s_{i+\frac{N}{2}} \\ s_{i+\frac{3N}{4}} \end{bmatrix} + \begin{bmatrix} n_i \\ n_{i+\frac{N}{4}} \\ n_{i+\frac{N}{2}} \\ n_{i+\frac{3N}{4}} \end{bmatrix} \right) = \begin{bmatrix} d_i^{(0)} \\ d_{i+\frac{N}{4}}^{(0)} \\ d_i^{(1)} \\ d_i^{(2)} \end{bmatrix} + \begin{bmatrix} z_i^{(0)} \\ z_{i+\frac{N}{4}}^{(0)} \\ z_i^{(1)} \\ z_i^{(2)} \end{bmatrix},$$

which would still allow pre-processing at CO because Φ^{-1} still exists. In this case, the three groups in Fig. 2 are able to receive 1/2 or 1/4 of the downstream data. This makes it possible to assign higher capacities to some ONUs thanks to the use of ADCs with higher sub-Nyquist rates, and lower capacities to other ONUs, thereby enhancing the design flexibility of heterogeneous DDM-OFDM-PONs. Due to the fact that the DDM scheme with either a fixed sub-Nyquist rate or hybrid sub-Nyquist rates is enabled by suitable variations in the sampling delays, however, the signal performance would be degraded with an inaccurate sampling delay at the receiver [5].

3. Experiments and Discussion

Fig. 3(a) illustrates the experiment setup. The optical transmitter was an electro-absorption modulated DFB laser (EML) operating at 1556 nm. When using off-line pre-processing, the electrical driving signals were generated by an arbitrary waveform generator (AWG, Keysight M8195A) with a sampling rate of 28 GSa/s. Using the FFT size of 2048, the OFDM signals occupied a bandwidth of 7 GHz, corresponding to a Nyquist rate of 14 GSa/s. We set the number of used subcarriers at 480 (excluding those that cannot be used in DDM [5]) and the cyclic prefix at 3/64, using a 16-QAM modulation format. An Erbium-doped fiber amplifier (EDFA) was inserted after the EML to enable 9-dBm launch power, and an optical bandpass filter (OBPF) was used to reduce out-of-band amplified spontaneous emission (ASE) noise. The input power of EDFA was -1 dBm, and the 3-dB

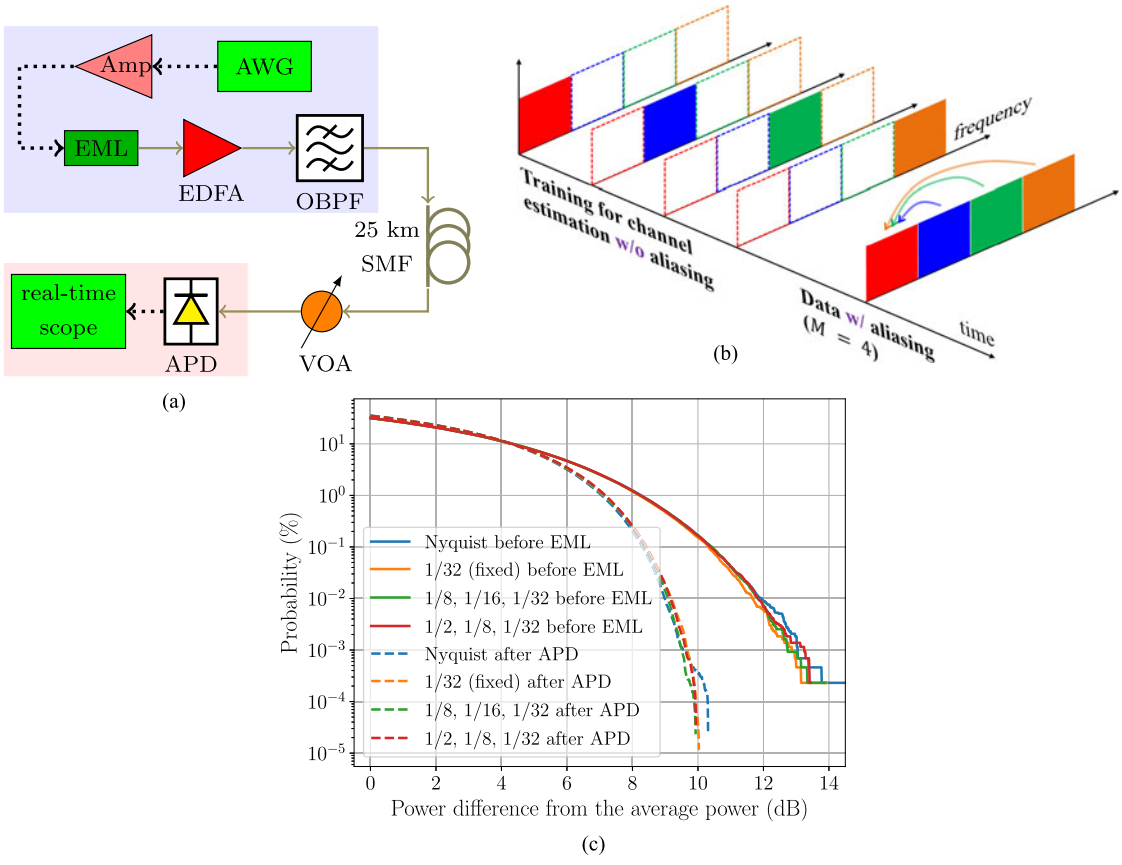

Fig. 3. (a) Experiment setup of proposed DDM-OFDM-PON, (b) design of training symbols for channel estimation using sub-Nyquist sampling, and (c) the measured CCDFs of PAPR.

bandwidth of OBPF was 1.3 nm. Following transmission over 25-km single-mode fiber (SMF), we used an APD (AT10EC-J57) to detect the OFDM signals. The DDM scheme reduces the requirement of sampling rate, but not the analog bandwidth of an ADC, making commercial ADCs with lower sampling rates not suitable in this work. Thus, instead of using ADCs with various sub-Nyquist rates, the received electrical signal was captured using a real-time oscilloscope (Keysight DSA-X 93204A) at a sampling rate of 80 GSample/s in conjunction with an off-line DSP to emulate the results obtained using hybrid sub-Nyquist rates in a consistent and simple manner. No additional signal process is required at the receiver; therefore, our DSP program deals only with resampling to sub-Nyquist rates and standard OFDM demodulation. To demonstrate the efficacy of the proposed system using hybrid sampling rates, we used three different sub-Nyquist sampling rates (i.e., $P = 3$) in a DDM-OFDM-PON with the following parameters: (i) $(1/M_0, 1/M_1, 1/M_2) = (1/2, 1/8, 1/32)$ and $(L_0, L_1, L_2) = (1, 2, 8)$ or (ii) $(1/M_0, 1/M_1, 1/M_2) = (1/8, 1/16, 1/32)$ and $(L_0, L_1, L_2) = (2, 4, 16)$. It should be noted that the channel response required for pre-processing was estimated using aliasing-free training symbols, despite the fact that we employed sub-Nyquist sampling. Fig. 3(b) illustrates the design of training symbols using the case of $M = 4$ as an example. Each training symbol is only composed of subcarriers localized in the Nyquist zone, wherein subcarriers in different frequency zones are sent sequentially to estimate the overall channel response without being affected by aliasing. To avoid any chance of aliasing during channel estimation in any of the ONUs, we designed the training symbols in accordance with the lowest sampling rate. Thus, training subcarriers in 32 different frequency zones were sent sequentially to enable channel estimation prior to the implementation of pre-processing. It should be also noted that the pre-processing in the proposed DDM scheme does not change the characteristics of peak-to-average power ratio

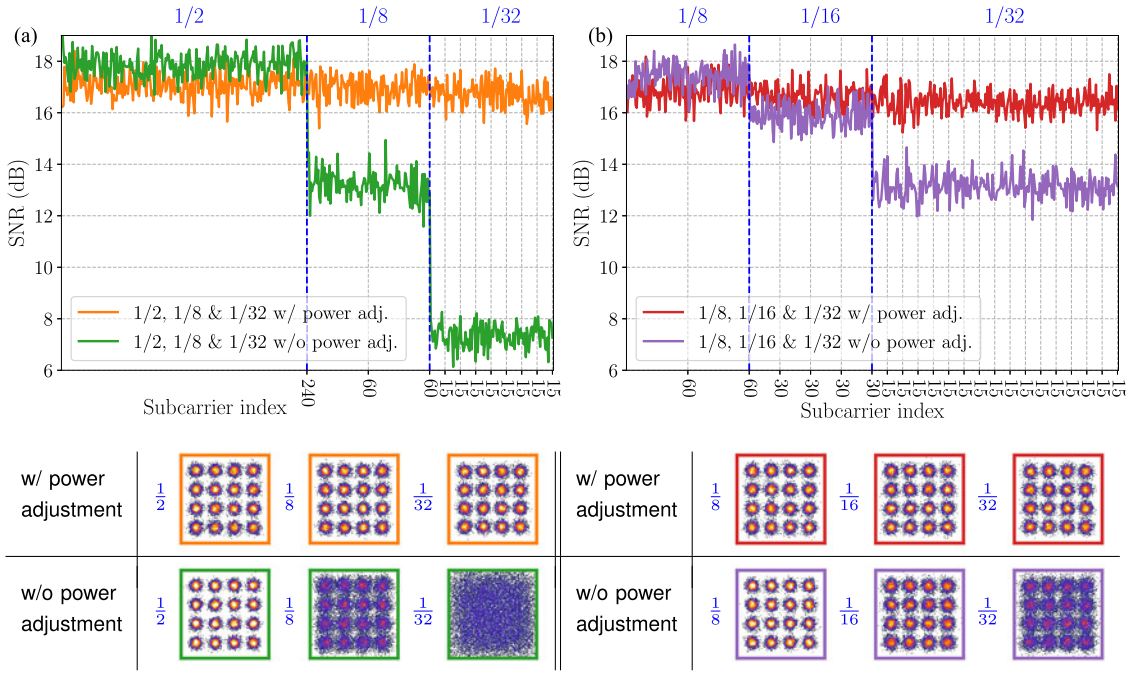

Fig. 4. Measured SNR following 25 km SMF, using hybrid sampling rates of (a) 1/32, 1/8, and 1/2 and (b) 1/32, 1/16, and 1/8 of Nyquist rate.

(PAPR), as shown in Fig. 3(c), where the complementary cumulative distribution functions (CCDFs) of PAPR were measured before the EML and after the APD. Thus, an additional requirement of digital-to-analog converter (DAC) is not needed at the transmitter in the proposed DDM-PON.

Fig. 4 presents the measured signal-to-noise ratio (SNR) at an optical received power of −18 dBm. Only a portion of the subcarriers are received when using sub-Nyquist sampling; therefore, all of the received subcarriers from all virtual groups are assembled, as shown in Fig. 4. The horizontal axis in Fig. 4(a) shows some of the ONUs received 240 or 60 subcarriers whereas the others received only 15. When the power of all received subcarriers (i.e., $d^{(m)}$ in (5)) were set at the same level in pre-processing (i.e., cases without power adjustment), the subcarriers with lower sampling rates had lower SNR. This can be explained by the fact that lower sampling rates increase the amount of spectral aliasing and noise (i.e., $z^{(m)}$), as shown in Fig. 2(b). As a result, the SNR values obtained at 1/8 and 1/32 of the Nyquist rate were respectively ∼6 and 12 dB lower than those obtained at 1/2 of the Nyquist rate in Fig. 4(a). Likewise, the SNR values obtained using 1/16 and 1/32 of the Nyquist rate were respectively ∼3 and 6 dB lower than those obtained at 1/8 of the Nyquist rate in Fig. 4(b). This situation necessitates power adjustment for $d^{(m)}$ during pre-processing, in order to equalize the performance of the various groups. Thus, our proposed modification to pre-processing is meant to make the subcarrier power levels inversely proportional to the sampling rates. For the example in (5) and Fig. 2, the required power adjustment is,

$$\begin{bmatrix} d_i^{(0)} \\ d_{i+\frac{N}{4}}^{(0)} \\ d_i^{(1)} \\ d_i^{(2)} \end{bmatrix} \xrightarrow{\text{power adjustment}} \begin{bmatrix} \sqrt{2} & 0 & 0 & 0 \\ 0 & \sqrt{2} & 0 & 0 \\ 0 & 0 & \sqrt{4} & 0 \\ 0 & 0 & 0 & \sqrt{4} \end{bmatrix} \begin{bmatrix} d_i^{(0)} \\ d_{i+\frac{N}{4}}^{(0)} \\ d_i^{(1)} \\ d_i^{(2)} \end{bmatrix}. \tag{6}$$

As shown in Fig. 4, following power adjustments in accordance with the sampling rates, the measured SNR values are similar in each of the groups. The corresponding constellations in Fig. 4 again illustrate the need for subcarrier power modification to equalize signal performance using different sub-Nyquist sampling rates.

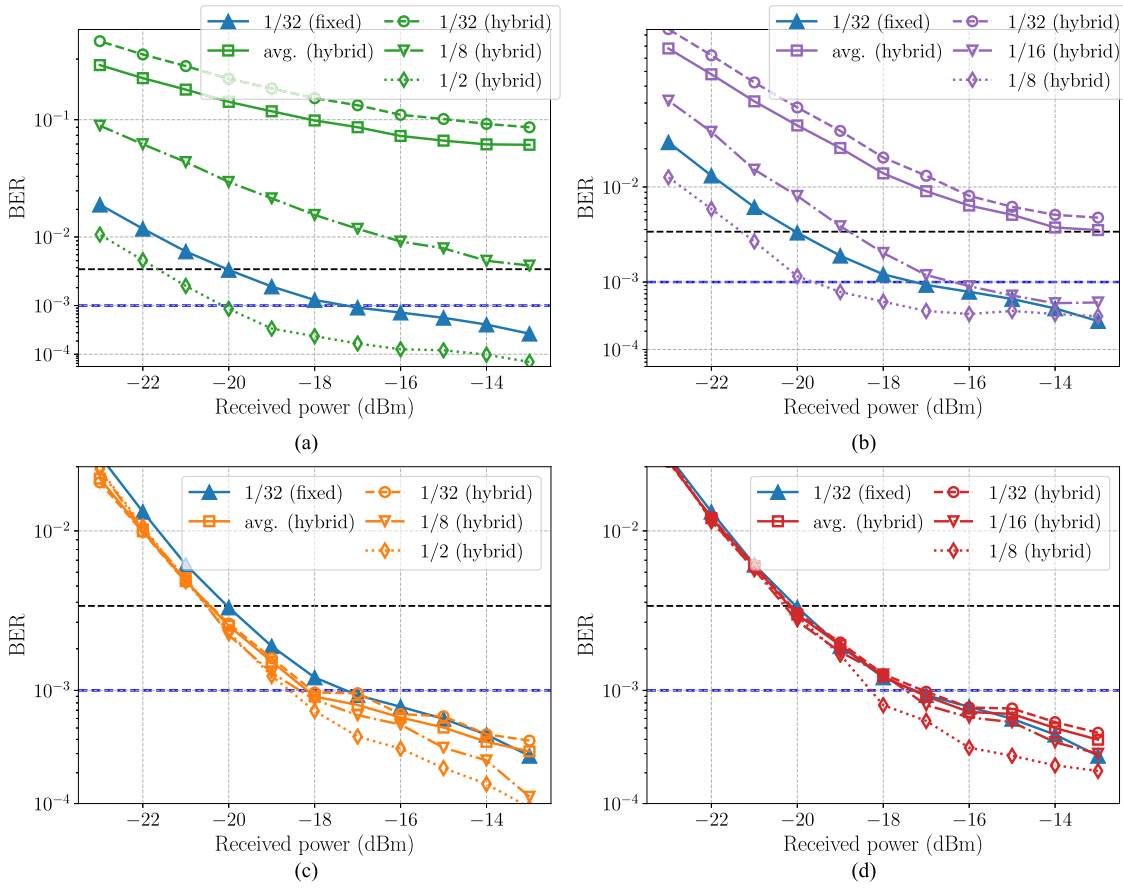

Fig. 5. Measured BER following 25 km SMF, using hybrid sampling at (a) 1/32, 1/8, and 1/2 of Nyquist rate without power adjustment, (b) 1/32, 1/16, and 1/8 of Nyquist rate without power adjustment, (c) 1/32, 1/8, and 1/2 of Nyquist rate with power adjustment, and (d) 1/32, 1/16, and 1/8 of Nyquist rate with power adjustment.

The measured bit-error rates (BERs) obtained using bit-by-bit comparison are plotted in Fig. 5. The results obtained using a fixed 1/32 of the Nyquist rate are plotted as reference. Without power adjustment, the average BER is far worse than that of the reference, thereby failing to reach the FEC limit at BER of 10^{-3}. The BER values obtained using specific sub-Nyquist sampling rates without power adjustment are plotted individually in Fig. 5(a) and (b). Clearly, the signals with the lowest sampling rate (i.e., 1/32 of Nyquist rate) failed to reach the FEC limit, and dominated the average BER performance. The comparison between Fig. 5(a) and (b) reveals that different combinations of sub-Nyquist samplings will lead to different BER performances by the same sampling rate. For instance, the detection using $1/8$ of Nyquist rate can achieve the sensitivity of -20 dBm in Fig. 5(b), but it cannot even reach the FEC limit in Fig. 5(a). This is because the total signal power is fixed and different combinations of sub-Nyquist samplings imply different relative powers for the signals with the same sampling rate. Moreover, as shown in Fig. 5(c) and (d), the signals with modified pre-processing present similar performance, with a difference in sensitivity of less than 1 dB. This is a clear demonstration that power adjustment is required during pre-processing to make signal performance insensitive to sampling rates. In this case, the average and individual BER values are similar to the BER values obtained using a fixed sub-Nyquist sampling rate, which resulted in sensitivity of better than -17 dBm at all sampling rates. However, a slightly better BER performance was observed as using a higher sampling rate in Fig. 5(c) and (d). The possible reason is the slight deviation in channel estimation and pre-processing, which could lead to more impact after more times of spectral superposition (i.e., the case with a lower sub-Nyquist rate). In spite of 1-dB

difference in sensitivity, the loss budget for all sampling rates reached 26 dB. To satisfy N1 class budget of 29 dB [11], however, a stronger FEC would be needed. For instance, if the FEC limit is set to 3.8×10^{-3} [12], the loss budget of 29 dB can be achieved, as shown in Fig. 5(c) and (d).

4. Conclusion

This paper reports on a novel DDM-OFDM-PON employing ADCs using different sub-Nyquist rates to enable flexible bandwidth sharing for heterogeneous ONUs. The sub-Nyquist sampling rates can be tailored to the bandwidth requirement of the ONU in the hybrid-sampling-rate DDM-OFDM-PON. Using the proposed pre-processing modification at CO makes it possible for the ONUs to receive data of various bandwidths at similar sensitivities. In experiments, we demonstrated 25-Gbps aggregated downstream, based on a hybrid sub-Nyquist sampling at 7, 1.75, and 0.44 (or 1.75, 0.88 and 0.44) GSa/s in 1, 2 and 8 (or 2, 4 and 16) virtual groups of ONUs, respectively, achieving exclusive data detection of 12.5, 3.13, and 0.78 (or 3.13, 1.56, and 0.78) Gbps with a 26-dB loss budget after 25-km SMF.

References

[1] N. Cvijetic, D. Qian, and J. Hu, "100 Gb/s optical access based on optical orthogonal frequency-division multiplexing," *IEEE Commun. Mag.*, vol. 48, no. 7, pp. 70–77, Jul. 2010.
[2] L. Mehedy, M. Bakaul, A. Nirmalathas, and S. Skafidas, "100 Gb/s 1024-way-split 100-km long-reach PON using spectrally efficient frequency interleaved directly detected optical OFDM," in *Proc. Quantum Electron. Conf. Lasers Electro-Opt*, 2011. pp. 1648–1650.
[3] M. C. Yuang *et al.*, "A high-performance OFDMA PON system architecture and medium access control," *J. Lightw. Technol.*, vol. 30, no. 11, pp. 1685–1693, 2012.
[4] C.-C. Wei, H.-C. Liu, and C.-T. Lin, "Novel delay-division-multiplexing OFDMA passive optical networks enabling low-sampling-rate ADC," in *Proc. Opt. Fiber Commun. Conf. Expo*, 2015. Paper M3J.1.
[5] C.-C. Wei, H.-C. Liu, C.-T. Lin, and S. Chi, "Analog-to-digital conversion using sub-Nyquist sampling rate in flexible delay-division multiplexing OFDMA PONs," *J. Lightw. Technol.*, vol. 34, no. 1, pp. 2381–2390, 2016.
[6] D. Qian, J. Hu, P. N. Ji, and T. Wang, "10-Gb/s OFDMA-PON for delivery of heterogeneous services," in *Proc. Optical Fiber Commun. Conf. Expo*, 2008. Paper OWH4.
[7] R. M. Ferreira, A. Shahpari, S. B. Amado, J. D. Reis, A. N. Pinto, and A. L. Teixeira, "Real-time flexible heterogeneous UDWDM system for coherent PON," in *Proc. Eur. Conf. Opt. Commun*, 2016. pp. 776–778.
[8] T. Orphanoudakis, E. Kosmatos, and J. Angelopoulos, "Exploiting PONs for mobile backhaul," *IEEE Commun. Mag.*, vol. 51, no. 2, pp. S27–S34, 2013.
[9] J. Li and J. Chen, "Passive optical network based mobile backhaul enabling ultra-low latency for communications among base stations view document," *J. Opt. Commun. Netw.*, vol. 9, no. 10, pp. 855–863, 2017.
[10] L. Zhou *et al.*, "Demonstration of software-defined flexible-PON with adaptive data rates between 13.8 Gb/s and 5.2 Gb/s supporting link loss budgets between 15 dB and 35 dB," in *Proc. Eur. Conf. Opt. Commun*, 2014. Paper P.7.24.
[11] D. T. van Veen and V. E. Houtsma, "Proposals for cost-effectively upgrading passive optical networks to a 25G line rate," *J. Lightw. Technol.*, vol. 35, no. 6, pp. 1180–1187, 2017.
[12] G. Raybon *et al.*, "High symbol rate coherent optical transmission Systems: 80 and 107 Gbaud," *J. Lightw. Technol.*, vol. 32, no. 4, pp. 824–831, 2014.